Solar Physics (2005) 230: 27–53

SORCE CONTRIBUTIONS TO NEW UNDERSTANDING OF GLOBAL CHANGE AND SOLAR VARIABILITY

JUDITH LEAN
E. O. Hulburt Center for Space Research, Naval Research Laboratory, Washington, DC, U.S.A.

and

GARY ROTTMAN, JERALD HARDER and GREG KOPP
Laboratory for Atmospheric and Space Physics, University of Colorado, Boulder, CO, U.S.A.

(Received 5 May 2005; accepted 23 June 2005)

Abstract. An array of empirical evidence in the space era, and in the past, suggests that climate responds to solar activity. The response mechanisms are thought to be some combination of direct surface heating, indirect processes involving UV radiation and the stratosphere, and modulation of internal climate system oscillations. A quantitative physical description is, as yet, lacking to explain the empirical evidence in terms of the known magnitude of solar radiative output changes and of climate sensitivity to these changes. Reproducing solar-induced decadal climate change requires faster and larger responses than general circulation models allow. Nor is the indirect climatic impact of solar-induced stratospheric change adequately understood, in part because of uncertainties in the vertical coupling of the stratosphere and troposphere. Accounting for solar effects on pre-industrial surface temperatures requires larger irradiance variations than present in the contemporary database, but evidence for significant secular irradiance change is ambiguous. Essential for future progress are reliable, extended observations of the solar radiative output changes that produce climate forcing. Twenty-five years after the beginning of continuous monitoring of the Sun's total radiative output, the Solar Radiation and Climate Experiment (SORCE) commences a new generation of solar irradiance measurements with much expanded capabilities. Relative to historical solar observations SORCE monitors both total and spectral irradiance with significantly reduced uncertainty and increased repeatability, especially on long time scales. Spectral coverage expands beyond UV wavelengths to encompass the visible and near-IR regions that dominate the Sun's radiative output. The space-based irradiance record, augmented now with the spectrum of the changes, facilitates improved characterization of magnetic sources of irradiance variability, and the detection of additional mechanisms. This understanding provides a scientific basis for estimating past and future irradiance variations, needed for detecting and predicting climate change.

1. Introduction

A balance between incoming solar radiation (with peak flux near 500 nm) and outgoing radiation from the much cooler terrestrial surface (with peak flux near 10 μm) establishes Earth's global mean temperature (e.g., Pilewskie and Rottman, 2005). When this radiative balance is perturbed, for example by a change in solar

radiation, atmospheric composition or surface reflectivity, Earth's surface temperature responds by seeking a new equilibrium. This response, which is in the range of 0.3 –1 °C per Wm^{-2} of forcing (Intergovernmental Panel on Climate Change, 2001) alters climate. Significant climate change can accompany even modest changes in global temperature. For example, during the last ice age 20 000 years ago, globally averaged temperatures were 5 °C cooler than at present; a response to forcing of 6.5 Wm^{-2} (Hansen, 2004).

As a part of NASA's Earth Observing System, the Solar Radiation and Climate Experiment (SORCE) seeks new understanding of the Sun's role in global change by measuring total and spectral solar irradiance, quantifying the solar sources of observed variations, and investigating the responses to these variations of Earth's climate and atmosphere (Rottman, 2005). Changes in solar electromagnetic radiation reaching Earth's surface perturb the radiative balance directly. Changes in solar UV radiation alter ozone and may have an indirect influence via coupling of the middle atmosphere with the surface by both radiative and dynamical processes (Haigh, 2001; Rind, 2002).

SORCE aims to specify daily total solar irradiance with an uncertainty of less than 100 ppm (0.01%) and repeatability of 0.001% per year, and daily solar ultraviolet irradiance from 120 to 300 nm with a spectral resolution of 1 nm, an uncertainty of better than ±5%, and repeatability of ±0.5%. These observations of total and UV spectral irradiance continue extant databases that now exceed, respectively, 27 and 14 years. SORCE is also making the first precise daily measurements of solar spectral irradiance between 0.3 and 2 μm with a goal of ±0.1% uncertainty and ±0.01% per year repeatability. These observations commence new databases of visible and near-IR solar irradiances. So that the SORCE observations may interface with the historical irradiance data and with future operational monitoring by the National Polar-orbiting Operational Environmental Satellite System (NPOESS), relationships must be identified with all concurrent, overlapping observations. Biases in absolute calibrations must be established and understood, as must differences in temporal trends among independent radiometers.

New understanding of the solar sources of the irradiance variations observed by SORCE permit improved models of contemporary irradiance variability. The parameterizations of the sunspot and facular sources in these models are the basis of reconstructions of past and future total and spectral irradiance changes. Reliable spectral irradiance time series enable more robust empirical and theoretical studies of Earth's surface, and ocean and atmospheric variability. Most studies conducted thus far have used proxies for solar variability, such as the 10.7 cm radio flux (e.g., Gleisner and Thejll, 2003; Labitzke, 2004), rather than the actual irradiances. Climate change simulations typically use total rather than spectral irradiance to specify solar forcing (e.g., Tett *et al.*, 2002; Meehl *et al.*, 2003). SORCE's spectral irradiance observations will enable more realistic climate model simulations for comparison with empirical evidence and projections of future change, in comparison with other climate influences.

2. Solar Influences on Global Change

New understanding of solar influences on global change is emerging from a variety of investigations. Empirical comparisons utilize databases that characterize the surface, ocean and atmosphere observationally; process studies seek to quantify mechanisms by which the Earth system responds to various forcings, and modeling simulations attempt to integrate the empirical evidence and the physical understanding. These efforts focus on three primary time scales – decadal variability in the current epoch of high quality observations, especially from space; centennial variability during the past millennium, for which actual temperature changes are known directly from measured records and indirectly from reconstructions (Jones and Mann, 2004); and centennial and millennial variability in the Holocene (e.g., Bond *et al.*, 2001).

2.1. Empirical evidence

Comprehensive records now exist for a multitude of climate forcings (solar irradiance, greenhouse gas and volcanic aerosol concentrations), feedbacks (cloud cover and cloud properties, water vapor), internal oscillations (El Niño-Southern Oscillation/ENSO, North Atlantic Oscillation/NAO, Quasi-Biennial Oscillation/QBO) and climate itself (surface temperatures, rainfall, circulation patterns), including the overlying atmosphere (temperature, ozone, geopotential heights, winds). The records of the past 25 years sample a range of natural and anthropogenic radiative forcing strengths and internal modes. The period includes the El Chichón and Pinatubo volcanoes, almost three solar activity cycles (including the most recent cycle free of volcanic interference), a few major ENSO events, and significant increases in greenhouse gases, chlorofluorocarbons (CFCs), and tropospheric (industrial) aerosols.

A linear combination of solar, anthropogenic (combined greenhouse gases and industrial aerosols), volcanic and ENSO influences can account for approximately 50% of the observed variance in global surface temperature (as reported by GISS, the Goddard Institute for Space Studies) between 1979 and 2004. Figure 1 compares the relative strength of each influence, derived from multiple regression analysis of monthly data. Hansen *et al.* (2002) describe the datasets. The total solar irradiance is that modeled by Lean (2000), the surface temperatures are combined land and ocean records, volcanic aerosols are from Sato *et al.* (1993), and ENSO is depicted by the Multivariate ENSO Index of Wolter and Timlin (1998).

According to the correlation coefficients listed in Table I, ENSO, solar and volcanic influences account for, respectively, 1.5, 4, and 13% of the monthly mean global surface temperature variance over this 25-year period. The anthropogenic influence accounts for a significantly larger 43%. The surface warms 0.1 °C at solar cycle maxima (forcing of 0.2 Wm^{-2}) and 0.39 °C overall from anthropogenic

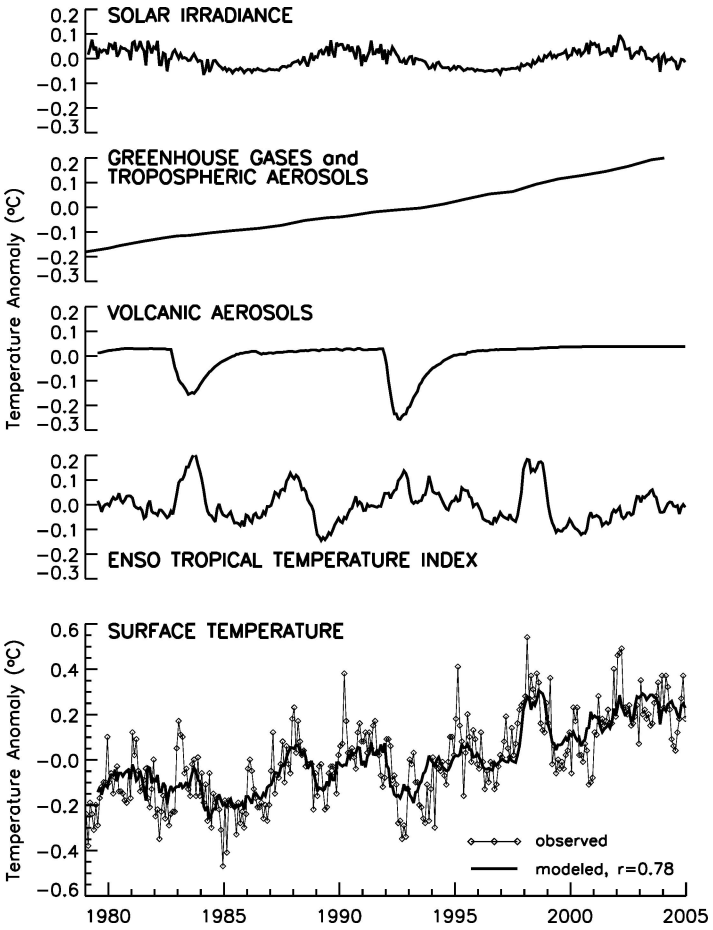

Figure 1. Comparison of different sources of variance in Earth's recent surface temperature, deduced from multiple regression analysis. The volcanic aerosols and ENSO indices are lagged by 6 months, and solar irradiance by 1 month, relative to the observed surface temperatures.

influences (forcing of $1\,\mathrm{Wm}^{-2}$). ENSO and volcanic activity produce episodic fluctuations that can exceed $0.2\,^{\circ}$C. Douglass and Clader (2002) reported similar results for lower tropospheric temperatures measured by the microwave sounding unit.

The solar signal in surface temperature shown in Figure 1 is consistent with other detections of decadal solar effects in the ocean (White, Dettinger, and Cayan, 2003) and atmosphere (van Loon and Shea, 2000; Coughlin and Tan, 2004; Labitzke, 2004), and with several independent analyses that further explore the meridional and height dependences of various forcings. Overall, the troposphere is warmer, moister, and thicker during solar maximum, with a distinct zonal signature. The strongest response occurs near the equator and at mid latitudes (40–$50\,^{\circ}$) with

TABLE I

Comparison of solar and other contributions to variance in monthly mean global surface temperatures in recent decades and in the past century.

Process	1979–2004 (306 months)	1882–2004 (1469 months)
Solar irradiance	0.211	0.506
Anthropogenic gases	0.654	0.801
Volcanic aerosols	−0.361	−0.137
ENSO	0.124	0.278
Model (all of above)	0.778	0.846

Listed are the correlations of the reconstructed components of individual processes with surface temperatures using the time series shown in Figures 1 and 2. Squared values give explained variance.

subtropical minima (Gleisner and Thejll, 2003). The primary surface temperature expression of these changes is warming in two mid-latitude bands (increases of 0.5 K at 20 – 60 ° N and S) that extend vertically to the lower stratosphere where they expand equatorward (Haigh, 2003). The patterns suggest that solar forcing invokes dynamical responses in the troposphere, involving the Hadley, Walker, and Ferrel circulation cells (Kodera, 2004; van Loon, Meehl, and Arblaster, 2004).

The relative influences of solar and other climate forcings are less certain prior to the era of space-based observations. Figure 2 and Table I compare relative strengths of ENSO, solar, volcanic and anthropogenic influences on monthly global surface temperatures between 1882 and 2004 using the parameterizations deduced after 1979. Together these influences account for 72% of the observed variance. In this figure, the MEI ENSO index is extended prior to 1950 by the Japan Meteorological Index. The solar component is obtained by reducing the background component in the total solar irradiance reconstruction of Lean (2000) to be consistent with the recent model of Wang, Lean, and Sheeley (2005) in which the secular increase is 27% that of earlier irradiance reconstructions (e.g., Lean, 2000; Fligge and Solanki, 2000). With this new irradiance model, the secular solar-induced surface temperature increase of 0.06 °C since 1880 is more than a factor of 10 smaller than the 0.7 °C warming attributed to anthropogenic influences. Solar-related global warming since the seventeenth century Maunder Minimum is of order 0.1 °C, or less, which is smaller than suggested by previous studies in which reconstructed solar irradiance changes were larger (Lean, Beer, and Bradley, 1995; Crowley, 2000; Rind *et al*., 2004).

Temperature responses to the solar cycle increase with altitude, from 0.1 K near the surface (Figure 1) to 0.3 K at 10 km, and 1 K around 50 km (van Loon and Shea, 2000). Accompanying the temperature changes is a solar cycle in global total ozone of ∼3% peak-to-peak amplitude. As with tropospheric climate, solar-induced

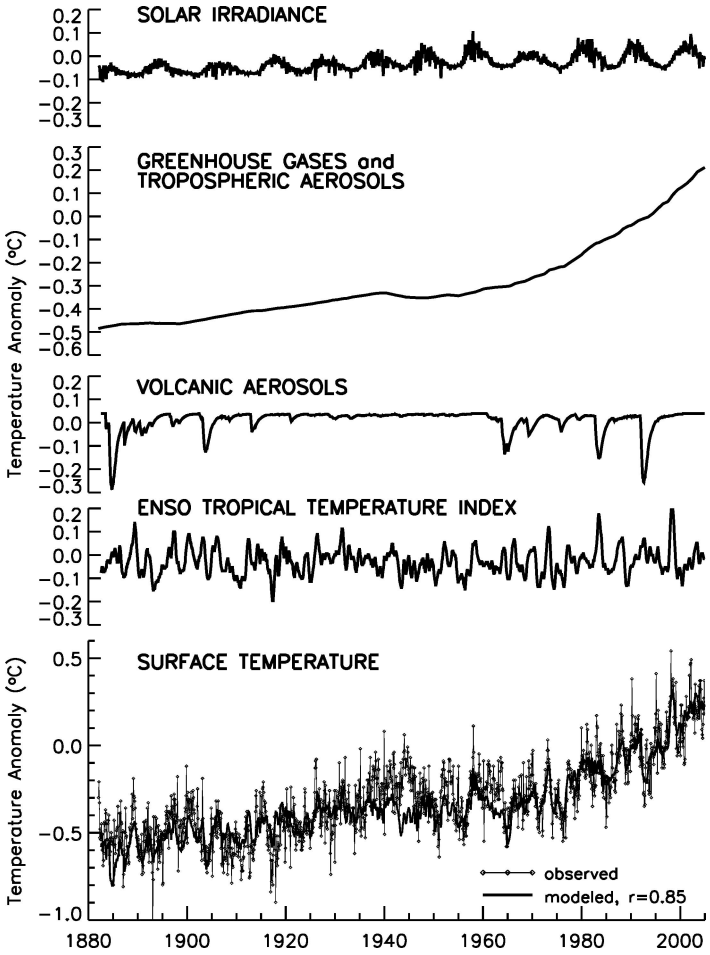

Figure 2. Shown are empirical estimates of the different sources of variance contributing to changes in the Earth's observed surface temperature during the past century, based on an extension of the multiple regression parameterizations in Figure 1.

changes in atmospheric temperature and composition occur simultaneously with anthropogenic effects and internal variability (e.g., QBO) (Jackman *et al.*, 1996; Geller and Smyshlyaev, 2002). Following the approach of McCormack *et al.* (1997) and Fioletov *et al.* (2002), Figure 3 illustrates the solar and other components of ozone variance extracted by statistical regression analyses of deseasonalized monthly total ozone from 1979 to 2004. Almost 80% of the total variance is explained by the combined effects of the QBO (9%), anthropogenic chlorofluorocarbons (39%), solar UV irradiance (42%) and volcanic (∼1%) activity. In this figure the ozone record is the Version 8 TOMS merged ozone dataset constructed by Goddard Space Flight Center, the QBO is the 30 mb zonal wind from the National Weather Service

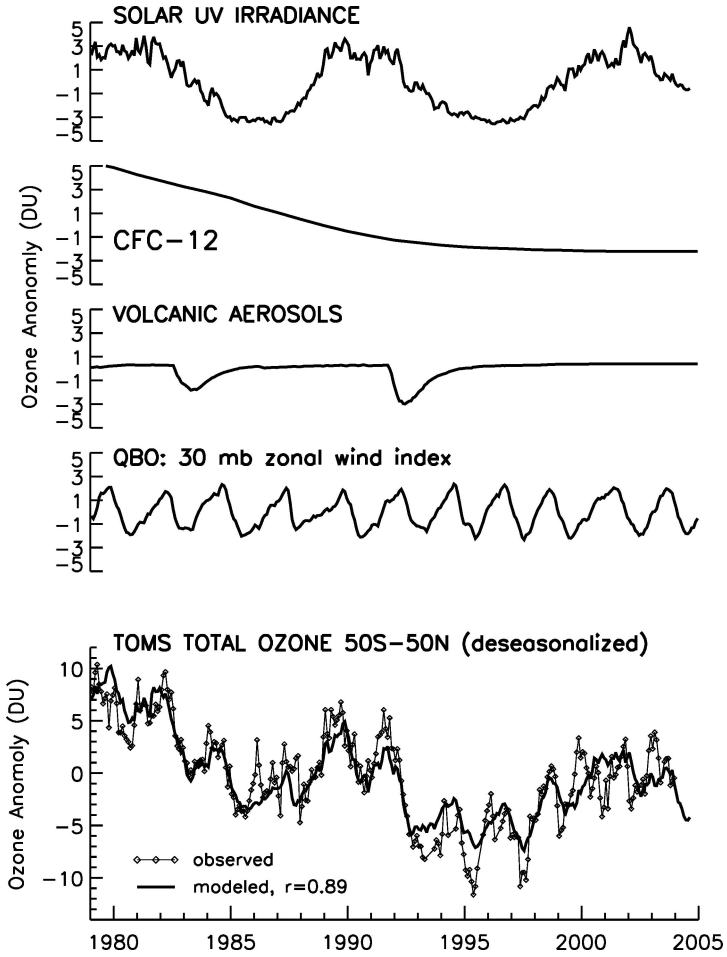

Figure 3. Comparison of difference sources of variance contributing to changes in observed, deseasonalized total ozone concentrations, deduced from multiple regression analysis.

Climate Prediction Center, and the UV irradiance is a band from 200 to 295 nm modeled by Lean (2000). The solar-induced ozone changes vary with geographical location and altitude in ways that are not clearly related linearly to the distribution of the forcing. For example, solar forcing appears to induce a significant and unexpected (from a modeling perspective) lower stratospheric response (Hood, 2003).

2.2. MECHANISMS

At least three distinct mechanisms are surmised for climate's response to solar radiative forcing. Irradiance changes in the near-UV, visible, and near-IR spectrum can

directly affect the Earth's radiative balance and surface temperature. Ultraviolet irradiance changes can alter the stratosphere whose coupling to the troposphere provides an indirect climate effect. Varying irradiance may interact with internal modes of climate variability (ENSO, NAO, and the QBO) and climate noise, triggering, amplifying or shifting the modes. Each mechanism is expected to have an individual geographical, altitudinal, and temporal response pattern.

An unequivocal determination of specific mechanisms has yet to be accomplished. As a result, alternate explanations are often proffered for common empirical evidence. For example, an apparent relationship between solar variability and cloud cover has been interpreted as a result of (1) sea surface temperatures altered directly by changing total solar irradiance (Kristjánsson *et al*., 2002), (2) solar-induced changes in ozone (Udelhofen and Cess, 2001), (3) internal variability by ENSO (Kernthaler, Toumi, and Haigh, 1999), and (4) changing cosmic ray fluxes modulated by solar activity in the heliosphere (Usoskin *et al*., 2004). In reality, different physical processes may operate simultaneously.

2.2.1. *Direct Surface Heating*

The near-UV, visible, and near-IR radiations that compose almost 99% of the Sun's total radiative output penetrate Earth's atmosphere to the troposphere and surface. Some 31% of the incident solar radiation is reflected back to space, the lower atmosphere absorbs 20%, and the surface and oceans absorb the remaining 49% (Kiehl and Trenberth, 1997). Geographical and seasonal inhomogeneities of this short-wave solar heating couple with land – ocean and cloud cover distributions to produce thermal contrasts that alter coupled land – atmosphere – ocean interactions (Rind and Overpeck, 1993; Meehl *et al*., 2003). As a result, the regional response to solar forcing may be significant even when the net global change is modest. The heating is thought to stimulate vertical motions that involve the Hadley cell and affect monsoons. The response may depend on the background state of the climate system, and thus on other forcings such as greenhouse gases (Meehl *et al*., 2003) and volcanic aerosols (Donarummo, Ram, and Stolz, 2002).

The empirical evidence suggesting a significant (0.1 K) surface temperature response to solar forcing (e.g., Figure 1), approximately in-phase with the solar cycle, is inconsistent with current understanding that oceanic thermal inertia strongly dampens (by a factor of 5) forcing at a period of the decadal solar cycle (Wigley and Raper, 1990). This suggests that the effect primarily involves the atmosphere and surface, but does not engage the deep ocean.

2.2.2. *Indirect Effects through the Stratosphere*

The Earth's atmosphere absorbs about 15 Wm^{-2} ($\sim$1%) of the Sun's radiant energy, in the ultraviolet portion of the spectrum. Solar UV radiation is more variable than total solar irradiance by at least an order of magnitude. It contributes significantly to changes in total solar irradiance (15% of the total irradiance cycle, Lean

et al., 1997) but is unavailable for direct forcing of climate because it does not reach the Earth's surface. Solar UV radiation creates the ozone layer (initially by photodissociating molecular oxygen in the atmosphere) and its effect on climate depends on the coupling of the stratosphere (where ozone primarily resides) with the troposphere (Haigh *et al*., 2004). Both radiative and dynamical couplings are surmised.

Because ozone absorbs electromagnetic radiation in the UV, visible, and IR spectral regions, changes in ozone concentration alter Earth's radiative balance by modifying both incoming solar radiation and outgoing terrestrial radiation. Solar-driven radiative coupling effects of this type may influence not only surface temperature (Lacis, Wuebbles, and Logan, 1990) but dynamical motions such as the strength of the Hadley cell circulation, with attendant effects on, for example, Atlantic storm tracks (Haigh, 2001). Because ozone controls solar energy deposition in the stratosphere, its variations alter both the altitudinal temperature gradient from the troposphere to the stratosphere, and the latitudinal gradient in the stratosphere, from the equator to the poles. These changes are postulated to propagate surface-wards through a cascade of feedbacks involving thermal and dynamical processes that alter winds and the large scale planetary waves (Rind, 2002). Equatorial winds in the stratosphere appear to play an important role in this process because of their impact on wind climatology (Matthes *et al*., 2004).

2.2.3. *Indirect Effects by Alteration of Internal Climate Variability*

Even with little or no global average response, solar radiative forcing may nevertheless influence climate by altering one or both of two main variability modes; ENSO (Neelin and Latif, 1998) and the NAO (Wallace and Thompson, 2002). Since the climate system exhibits significant "noise" the forcing may be amplified by stochastic resonance (Ruzmaikin, 1999). Also possible is the non-linear interaction of the forcing with existing cyclic modes. Such frequency modulation has been demonstrated on Milankovitch time scales (Rial, 1999).

Positive radiative forcing, including by solar variability, may suppress the frequency and occurrence of ENSO (Mann *et al*., 2005) because of sea surface temperature gradients arising from the deeper thermocline in the west Pacific Ocean relative to the east. Solar UV irradiance changes may alter the high latitude stratospheric and the polar vortex, thereby affecting the NAO (Shindell *et al*., 2003), which is observed to expand longitudinally to the Artic annual oscillation during solar maxima (Kodera, 2002). The phase of the quasi-biennial oscillation in stratospheric equatorial winds possibly modulates this interaction (Ruzmaikin and Feynman, 2002). That the phase of the QBO changes with the solar cycle (McCormack, 2003; Salby and Callaghan, 2004), as part of a pattern of non-linear stratospheric response to the 11-year cycle involving both the QBO and the SAO, underscores the complicated, multifaceted nature of solar influences on global change.

3. Solar Irradiance Variability

Empirical studies such as those in Figures 1–3, and theoretical investigations of climate processes and change, require reliable knowledge of solar spectral irradiance on multiple time scales. Continuous space-based measurements with adequate precision to detect real variations in total irradiance exist since 1978, in UV irradiance since 1991 and in visible and near-IR irradiance since 2003. For prior periods and future projections, irradiance variations are estimated using models that account for the changes observed in the contemporary era, in combination with proxies of solar activity recorded in the past and predicted for the future.

3.1. Observations

3.1.1. *Total Irradiance*

Four space-based instruments measure total solar irradiance at the present time. SORCE's Total Irradiance Monitor (TIM) (Kopp, Lawrence, and Rottman, 2005), together with the radiometers of the Variability of Irradiance and Gravity Oscillations (VIRGO) experiment on the Solar Heliospheric Observatory (SOHO), the ACRIM III on the Active Cavity Radiometer Irradiance Monitor Satellite (ACRIMSAT), and the Earth Radiation Budget Satellite (ERBS), contribute to a database that is uninterrupted since November 1978. Figure 4 compares three composite irradiance records obtained from different combinations of measurements. While the gross temporal features are clearly very similar, the slopes differ, as do levels at solar activity minima (1986 and 1996).

Secular trends differ among the three composite irradiance records because of different cross-calibrations and drift adjustments applied to individual radiometric sensitivities. The PMOD composite (Fröhlich and Lean, 2004) combines the observations by the ACRIM I on the Solar Maximum Mission (SMM), the Hickey–Friedan radiometer on Nimbus 7, ACRIM II on the Upper Atmosphere Research Satellite (UARS), and VIRGO on SOHO by analyzing the sensitivity drifts in each radiometer prior to determining radiometric offsets. In contrast, the ACRIM composite (Willson and Mordvinov, 2003), which utilizes ACRIMSAT rather than VIRGO observations in recent times, cross-calibrates the reported data assuming that radiometric sensitivity drifts have already been fully accounted for. For the Space Absolute Radiometric Reference (SARR) composite, individual absolute irradiance measurements from the shuttle are used to cross-calibrate satellite records (Dewitte *et al*., 2005).

Solar irradiance levels are likely comparable in the two most recent cycle minima when absolute uncertainties and sensitivity drifts in the measurements are assessed (Fröhlich and Lean, 2004). The upward secular trend of 0.05% proposed by Willson and Mordvinov (2003) may be of instrumental rather than solar origin. This irradiance "trend" is not a slow secular increase but a single episodic increase between

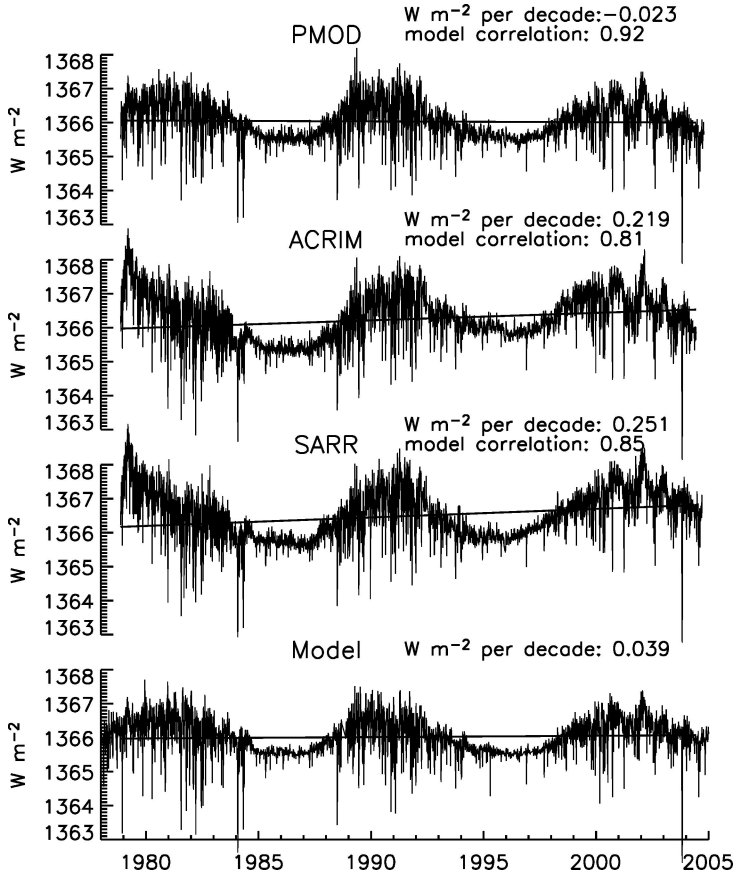

Figure 4. Shown in the *upper three panels* are different composite records of total solar irradiance during the era of space-based monitoring. For quantitative comparison, the slopes of the time series are computed from 7538 daily values between November 1978 and June 2004. Compared in the *bottom panel* is a model of total solar irradiance calculated from parameterized sunspot and facular influences.

1989 and 1992 that is present in the Nimbus 7 data. Independent, overlapping ERBS observations do not show a comparable increase at this time (Lee III *et al*., 1995). The trend is absent in the PMOD composite, in which total irradiance at successive solar minima is constant to better than 0.01%. Although a long-term trend is present in the SARR composite, the increase of 0.15 Wm^{-2} between successive solar activity minima (in 1986 and 1996) is not significant because the uncertainty is $\pm 0.35\ Wm^{-2}$.

SORCE's TIM observations, shown in Figure 5, aim at reducing such instrumental uncertainties in the long-term irradiance record. Table II compares TIM's mean irradiance and standard deviation with each of the irradiance time series in Figure 4 for the duration of the SORCE mission thus far. On average, TIM measures

TABLE II

Compared are absolute values, standard deviations, and trends of TIM observations with the three composite irradiance records and the empirical model in Figure 4, during the SORCE mission thus far (415 common daily values from 2003.15 to 2004.44).

TSI record	Mean value (Wm^{-2})	Standard deviation (Wm^{-2})	Ratio to TIM	Correlation with TIM	Slope (Wm^{-2} per year)
TIM	1360.98	0.579	1	1	−0.182 (0.013%)
PMOD	1365.76	0.573	1.00351	0.9964	−0.134 (0.010%)
ACRIM	1366.09	0.582	1.00375	0.9829	−0.261 (0.019%)
SARR	1366.73	0.577	1.00423	0.9967	−0.191 (0.014%)
Model	1365.95	0.479	1.00365	0.9634	−0.069 (0.005%)

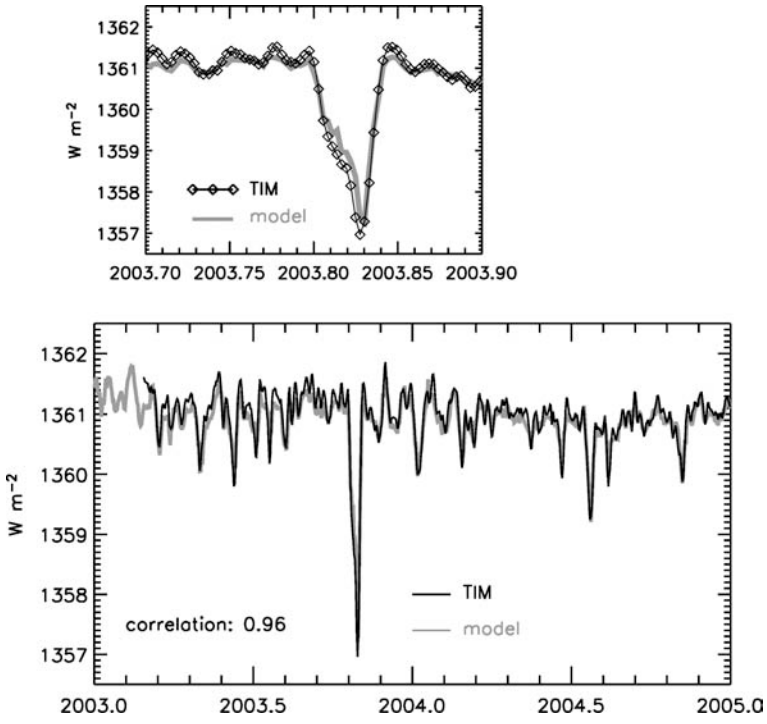

Figure 5. Shown are the TIM daily mean observations (symbols with *dark line*), compared with an empirical variability model developed from sunspot and facular influences (Lean, 2000). In the *upper panel* the observations and model are compared during the period of high solar activity in October 2003. In the *lower panel* the observations and model are shown for the duration of the SORCE mission thus far.

absolute solar irradiances 5.2 Wm^{-2} (0.4%) lower than the other radiometric time series. This difference is an order of magnitude larger than the combined uncertainties claimed for the respective measurements (e.g., ±0.01% for SORCE; ±0.025% for SARR) and the discrepancy is under investigation.

Standard deviations in Table II, which primarily reflect true solar irradiance variations, are on average comparable (∼0.04%) in TIM and the PMOD, ACRIM and SARR composites records. The notably different irradiance trends from 2003.15 to 2004.44 likely arise from residual instrumental drifts in the reported measurements. During this time of overall decreasing solar activity with the approach of solar minimum, TIM's downward slope is 1.55 times that of the PMOD composite, but 0.57 times that of the ACRIM composite.

3.1.2. *Spectral Irradiance*

With its Spectral Irradiance Monitor (SIM, Harder *et al*., 2005) and Solar Stellar Irradiance Comparison Experiment (SOLSTICE, McClintock, Rottman, and Woods, 2005), SORCE monitors the Sun's spectral irradiance almost simultaneously across ultraviolet, visible, and near-IR regions, for the first time from space on a daily basis with sufficient precision to detect real changes.

The overlap in time and wavelength of the SORCE SOLSTICE UV measurements with those made since 2000 by the EUV Grating Spectrometer on the Thermosphere Ionosphere Mesosphere Energetics and Dynamics (TIMED) spacecraft (Woods *et al*., 2005) extends spectral irradiance information to extreme ultraviolet wavelengths. The X-ray photometer systems on SORCE (Woods and Rottman, 2005) and TIMED complete the spectral coverage. In the UV spectrum, SORCE continues the spectral irradiance observations made since October 1991 by an earlier SOLSTICE instrument and the Solar Ultraviolet Spectral Irradiance Monitor (SUSIM), both flown on the Upper Atmosphere Research Satellite (Woods *et al*., 1996).

The comprehensive spectral coverage of the SORCE instruments provides unprecedented characterization of solar irradiance variability. As expected, variations occur at all wavelengths. The comparisons in Figure 6 and Table III illustrate the changes in the solar spectrum accompanying the increase in solar activity from 17 to 30 October 2003. During this time, the Sun's visible surface, shown in Figure 7, evolved from being almost sunspot free, to having significant sunspot coverage. At the same time, total solar irradiance is seen in Figure 5 to decrease by 4 Wm^{-2} (0.3%). The middle panel in Figure 6 shows the corresponding decreases in spectral irradiance energy, while the lower panel shows the fractional changes. Maximum energy changes occur at wavelengths from 400 to 500 nm, whereas fractional changes, listed numerically in Table III are greatest at UV wavelengths, where the energy change is, however, considerably smaller.

Radiation in the UV spectrum has a notably different temporal character during solar rotation than the spectrum above 300 nm, as the time series in Figure 8 illustrate. The standard deviation of the 200–300 nm time series in Figure 8 is 0.15%,

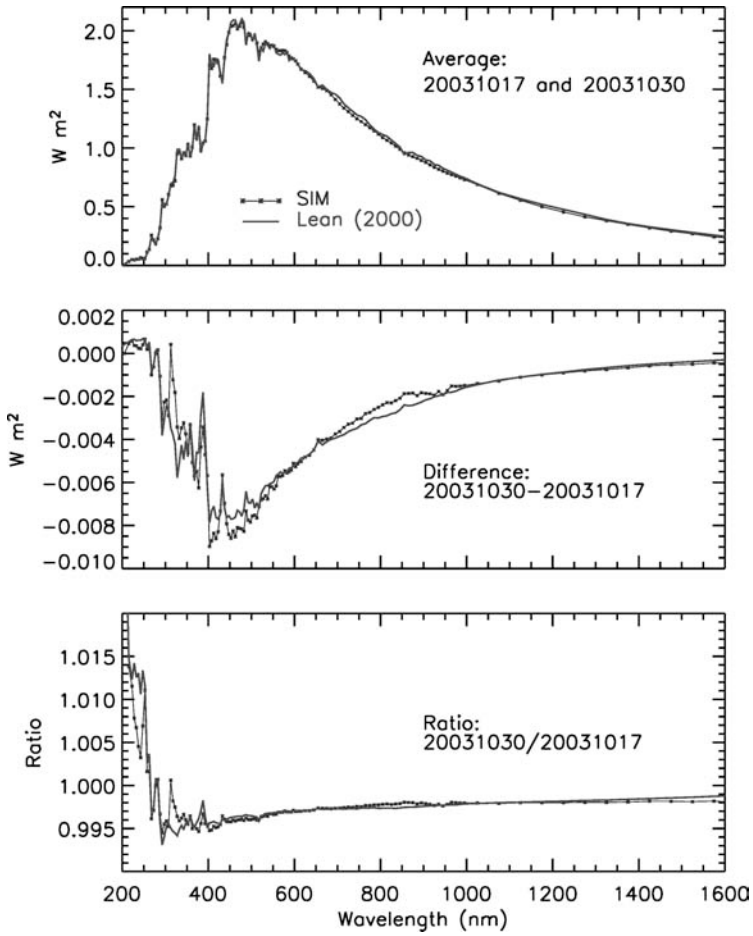

Figure 6. The solar spectral irradiance measured by SIM on SORCE, shown in the *upper panel*, is the average of two spectra, on 17 and 30 October 2003. Spectral irradiance changes caused by significant solar activity on 30 October, relative to quieter conditions on 17 October, are shown in the *middle panel* as energy differences, and the *lower panel* as fractional changes. A model of the irradiance variations caused by sunspots and faculae is compared with the SORCE observations.

decreasing to 0.04% for radiation in the wavelength band from 400 to 700 nm, and to 0.03% at 1000 to 1600 nm. These differences reflect the different solar origins of irradiance variability since the observations relate to emission from a range of temperatures and structures within solar atmosphere.

3.2. MODELS

3.2.1. *Present*

Two decades of solar observations and analysis have established the primary roles of sunspots and faculae in causing solar irradiance to vary (Fröhlich and Lean, 2004).

TABLE III

Variations in spectral irradiance bands during the strong solar rotation of October 2003, observed by SORCE and estimated from a model of facular and sunspot influences.

Spectral band (nm)	SORCE rotation 30 Oct 2003/ 17 Oct 2003	Model rotation 30 Oct 2003/ 17 Oct 2003	Model solar cycle 1989/1986	Model secular change 1713/1986 (Wang, Lean, and Sheeley, 2005)	Model secular change 1713/1986 (Lean, 2000)
200–300	0.9990	0.9993	1.013	0.9957	0.9864
315–400	0.9959	0.9956	1.002	0.9990	0.9968
400–700	0.9965	0.9967	1.0008	0.9995	0.9983
700–1000	0.9979	0.9975	1.0004	0.9997	0.9990
1000–1600	0.9980	0.9982	1.00025	0.9998	0.9994

The modeled changes are also given for the solar cycle (Lean *et al*., 1997) and Maunder Minimum, for which the recent estimates of Wang, Lean, and Sheeley (2005) are compared with earlier estimates of Lean (2000).

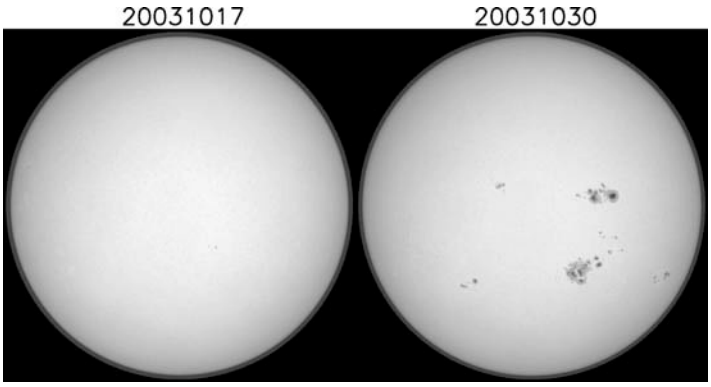

Figure 7. Continuum-light solar images made by the Michelson Doppler Imager instrument on SOHO are compared for 17 and 30 October 2003, the two days of the solar spectra compared in Figure 6.

Sunspots deplete the Sun's local emission so that their presence on the disk reduces irradiance, especially in the visible and infrared spectral regions. TIM and SIM record irradiance fluctuations that are the net effect of sunspot-induced reductions and facular-induced enhancement. The two influences compete continually as active regions emerge, evolve and decay on the solar surface, altering the relative strengths and phase of the sunspot and facular emissions (Rottman *et al*., 2005).

SORCE instruments observed the dramatic effects of active regions on irradiance when sunspot darkening increased dramatically and faculae brightening more modestly from 17 to 30 October 2003 (Figures 7 and 9). Total solar irradiance decreased 4 Wm^{-2} (Figure 5), as exceptionally large sunspots transited the Earth-facing solar disk (Figure 7). As Figure 6 shows, the sunspots depleted the entire solar spectrum at wavelengths between 350 and 1600 nm.

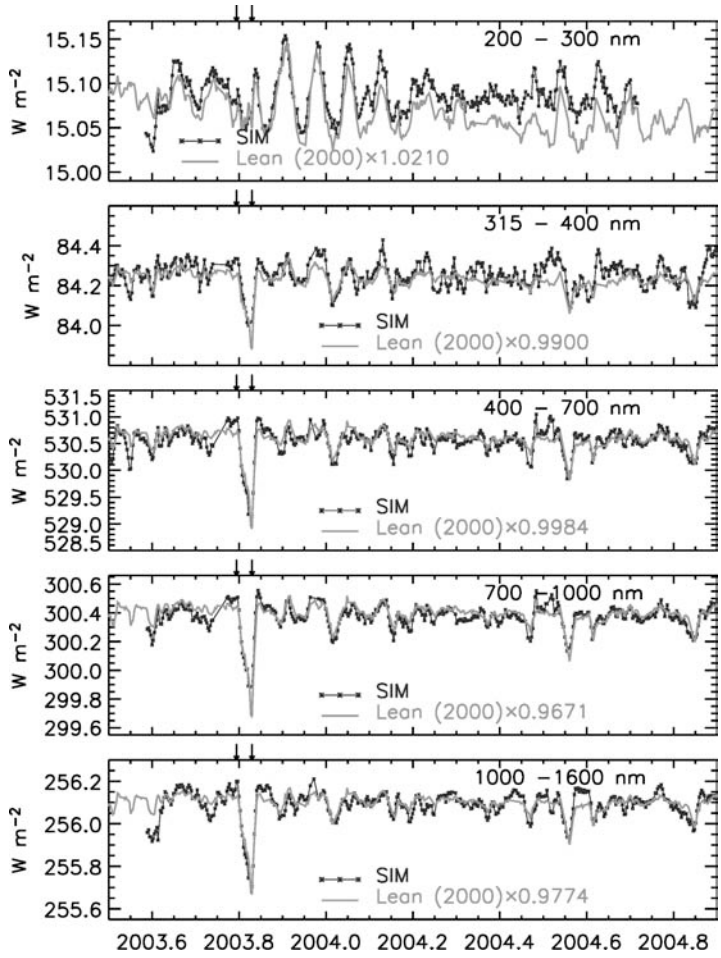

Figure 8. Compared are SORCE observations (*symbols*) and empirical variability model values (*solid line*) of irradiance in the: (a) middle ultraviolet, 200–300 nm, (b) near-UV, 315–400 nm, (c) visible, 400–700 nm, (d) visible, 700–1000 nm, and (e) near-IR, 1000–1600 nm wavelength bands. SORCE observations are made by SIM, except at wavelengths between 200 and 210 nm, which are made by SOLSTICE. The SORCE time series have been detrended by subtracting a 30-day running mean, to remove known instrumental drifts not yet incorporated in the data reduction algorithms. The model time series are scaled by the values shown in each panel to agree with the SIM absolute scale. Table III lists fractional changes of the time series from 17 to 30 October 2003 (indicated by the *arrows*).

Models that quantify the sunspot and facular influences on solar irradiance have been developed using a variety of approaches. Typically, the sunspot component is calculated directly using information about the location and size of all sunspots on the disk, obtained from visible images (Lean *et al.*, 1998), magnetograms (Krivova *et al.*, 2003), or images at other wavelengths (Preminger, Walton, and Chapman, 2002). More diverse is the approach for estimating brightness enhancements in

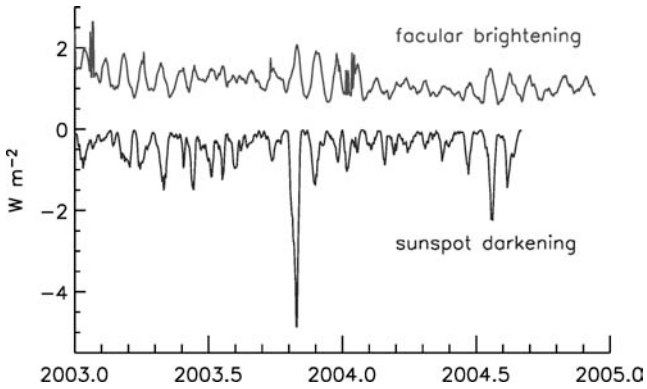

Figure 9. Shown are variations in the bolometric faculae brightening (*upper curve*) and sunspot darkening (*lower curve*) that together produce changes in total solar irradiance observed by TIM. The combination of these competing effects produces the modeled irradiance in Figure 5. Linear scalings that determine the relative contributions of the sunspots and facular are obtained from multiple regression of these time series with the PMOD composite in Figure 4.

faculae, which have lower contrasts and are more widely dispersed over the solar disk than are sunspots. Because photospheric faculae usually underlie bright chromospheric active regions, Ca II K images are often used (Lean *et al.*, 1998; Walton, Preminger, and Chapman, 2003). So too are fluxes of the Ca II and Mg II chromospheric emission lines (Lean, 2000; Fröhlich and Lean, 2004). More physical approaches for modeling irradiance are also being developed using magnetograms, precise solar photometry (Kuhn, Lin, and Coulter, 1999), and spectral synthesis techniques that seek to represent the intensity of a range of disk features as functions of wavelength and disk position (Fontenla *et al.*, 1999).

A model that linearly combines sunspot and facular effects is seen in Figure 5 to provide close (but imperfect) tracking of total irradiance variations recorded by TIM during October 2003, and in the SORCE mission thus far, accounting for 92% of observed variance. The model uses an estimate of sunspot darkening calculated explicitly from information about sunspot areas and locations recorded from white-light solar images (archived by NOAA in the National Geophysical Data Center), together with adopted center-to-limb functions and bolometric contrast (Lean *et al.*, 1998). Facular brightening is represented by the Mg II chromospheric index (Viereck *et al.*, 2004). Multiple regression of the sunspot darkening and facular proxy time series with the PMOD total solar irradiance composite (Figure 4) establishes the relative strengths of the sunspot and facular influences, as shown in Figure 9. According to the model, the 4 Wm^{-2} total irradiance reduction in October 2003 is the net effect of a 5 Wm^{-2} irradiance depletion by sunspot darkening, compensated by a 1 Wm^{-2} enhancement in bright facular emission.

The quantitative comparison summarized in Table II suggests that on average the total irradiance model underestimates the strength of both the facular and sunspot

influences on solar rotation time scales. This is evident visually in Figure 5, where the model irradiance is seen to be slightly lower than the observations during facular increases, and slightly higher during times of large sunspot reductions. It is also evident when compared statistically with all three composite time series during the past 26 years; the model's standard deviation of 0.038% is uniformly smaller than that of the observations (0.042% for PMOD, 0.051% for ACRIM, 0.053% for SARR). Model revisions are in progress to increase the modeled variance by revising the bolometric sunspot and facular parameterizations, and to investigate the model's underestimate of the overall downward total irradiance trend from 2003.15 to 2004.44 (Table I), possibly related to the Mg II facular index.

Relative spectral irradiance changes modeled by incorporating the spectral dependence of the sunspot and facular contrasts (Lean, 2000) are shown in Figure 6. The overall agreement is surprisingly good, since the modeled wavelength dependence is based on limited measurements of sunspot contrasts (Allen, 1981) and theoretical calculations of sunspot and facular contrasts (Solanki and Unruh, 1998). Nevertheless distinct differences are evident. From 17 to 30 October 2003, the model predicts energy changes that are smaller than observed at wavelengths from 400 to 500 nm, and larger than observed at wavelengths from 700 to 1000 nm. Nor are the variations of the spectral features in the region 300 to 400 nm modeled exactly. A particular deficiency is in the spectral region near 1.6 μm where the models appear to underestimate facular brightness (Fontenla *et al.*, 2004). By clearly delineating deficiencies in spectral irradiance models, the SORCE measurements are facilitating model improvements, such as in the wavelength dependence of the sunspot and facular contrasts and their relative temporal influences.

3.2.2. *Past*

Observations and models of irradiance (such as those shown in Figures 4–6 and 8) provide a scientific basis for reconstructing past solar irradiance. Proxy indicators of solar activity such as the *aa* index (Lockwood and Stamper, 1999), cosmogenic isotopes in tree-rings and ice-cores (Baud *et al.*, 2000), and the range of variability in Sun-like stars (Baliunas and Jastrow, 1990) place current solar activity levels in a broader context. The irradiance reconstructions of Hoyt and Schatten (1993), Lean, Beer, and Bradley (1995), Lean (2000), Lockwood and Stamper (1999), and Fligge and Solanki (2000) assume that longer term irradiance variations are larger than during the 11-year cycle, since the proxies suggest that the Sun is capable of a greater range of activity than witnessed during recent times. With this approach, total irradiance during the seventeenth century Maunder Minimum is reduced in the range of 0.15– 0.4% (2–5 Wm^{-2}) below contemporary cycle minima values. Table IV summarizes different estimates.

New studies (Lean, Wang, and Sheeley, 2002; Foster, 2004; Foukal, North, and Wigley, 2004; Wang, Lean, and Sheeley, 2005) raise questions about the proper interpretation of the proxies, and suggest that long-term irradiance changes are a

TABLE IV

Compared are estimates of the reduction in total solar irradiance during the Maunder Minimum relative to contemporary solar minimum.

Reference	Assumptions and technique	Maunder Minimum irradiance reduction (global climate forcing) from contemporary minimum (Wm^{-2})
Schatten and Orosz (1990)	11-Year cycle extrapolation	∼0.0 (0)
Lean, Skumanich, and White (1992)	No spots, plage, network in Ca images	1.5 (0.26)
Lean, Skumanich, and White (1992)	No spots, plage, network, and reduced basal emission in cell centers in Ca images non-cycling stars	2.6 (0.45)
Hoyt and Schatten (1993)*	Convective restructuring implied by changes in sunspot umbra/penumbra ratios	3.7 (0.65)
Lean, Beer, and Bradley (1995)	Non-cycling stars	2.6 (0.45)
Fligge and Solanki (2000)*	Combinations of above	4.1 (0.72)
Lean (2000)	Non-cycling stars (revised solar stellar calibration)	2.2 (0.38)
Foster (2004) Model No. 1	Non-magnetic Sun estimates by removing bright features from MDI images	1.6 (0.28)
Foster (2004) Model No. 3	Extrapolated from fit of 11-year smoothed total solar irradiance composite	0.8 (0.14)
Solanki and Krivova (2005)	Accumulation of bright sources from simple parameterization of flux emergence and decay	2.2 (0.38)
Wang, Lean, and Sheeley (2005)*	Flux transport simulations of total magnetic flux evolution	0.5 (0.09)

The solar activity cycle of order 1 Wm^{-2} is superimposed on this decrease. The climate forcing is the irradiance change divided by 4 (geometry) and multiplied by 0.7 (albedo). Reconstruction identified by * extend only to 1713, the end of the Maunder Minimum.

factor of 3 – 4 less (see Table IV). A reassessment of the stellar data has been unable to recover the original bimodal separation of (lower) Ca emission in non-cycling stars (assumed to be in Maunder Minimum type states) compared with (higher) emission in cycling stars (Hall and Lockwood, 2004) which underpins the Lean, Beer, and Bradley (1995) and Lean (2000) irradiance reconstructions. Long-term instrumental drifts may affect the *aa* index (Svalgaard, Cliver, and Le Sager, 2004) on which the Lockwood and Stamper (1999) irradiance reconstruction is based.

Nor do long-term trends in the *aa* index and cosmogenic isotopes (generated by open flux) necessarily imply equivalent long-term trends in solar irradiance (which track closed flux) according to simulations of the transport of magnetic flux on the Sun and propagation of open flux into the heliosphere (Lean, Wang, and Sheeley, 2002; Wang, Lean, and Sheeley, 2005).

Past solar irradiance has recently been reconstructed on the basis of solar considerations alone, without invoking geomagnetic, cosmogenic, or stellar proxies. From the identification of bright faculae in solar visible images made by the Michelson Doppler Imager (MDI) on SOHO, Foster (2004) estimates that removing all bright faculae reduces solar irradiance by $1.6\,\mathrm{Wm}^{-2}$ (see Table IV). This estimate of the irradiance of the "non-magnetic" Sun is consistent with an earlier estimate of Lean, Skumanich, and White (1992), who inferred a reduction of $1.5\,\mathrm{Wm}^{-2}$ from a similar analysis of solar Ca K images and fluxes (removal of all network but no alteration of basal cell center brightness). Both the Foster (2004) and Lean, Skumanich, and White (1992) approaches suggest that were the Maunder Minimum irradiance equivalent to the "non-magnetic" Sun, then the irradiance reduction from the present would be about half that of earlier estimates (see Table IV).

Using a quite different approach, Wang, Lean, and Sheeley (2005) also suggest that the amplitude of the background component is significantly less than has been assumed, specifically 0.27 times that of Lean (2000). This alternate estimate emerges from simulations of the eruption, transport, and accumulation of magnetic flux since 1713 using a flux transport model with variable meridional flow (Wang, Lean, and Sheeley, 2005). Both open and total flux variations are estimated, arising from the deposition of bipolar magnetic regions (active regions) and smaller-scale ephemeral regions on the Sun's surface, in strengths and numbers proportional to the sunspot number. The open flux compares reasonably well with the geomagnetic and cosmogenic isotopes which gives confidence that the approach is plausible. A small accumulation of total flux (and possibly ephemeral regions) produces a net increase in facular brightness which, in combination with sunspot blocking, permits the reconstruction of total solar irradiance shown in Figure 10. The increase from the Maunder Minimum to the present-day quiet Sun is $\sim 0.5\,\mathrm{Wm}^{-2}$ (Table IV), i.e., about one-third the reduction estimated for the 'non-magnetic" Sun.

Based on current physical understanding, the most likely long-term total irradiance increase from the Maunder Minimum to current cycle minima is therefore in the range 0.5–$1.6\,\mathrm{Wm}^{-2}$. The larger amplitude secular irradiance changes of the initial reconstructions are likely upper limits. Figure 11 shows modeled changes in the spectral irradiance bands of Figure 8 that correspond to the Wang, Lean, and Sheeley (2005) flux transport simulations. The model changes were obtained by using a background component 27% of that adopted in the spectral irradiance reconstructions of Lean (2000), which extend from 1610 to the present. In Table III are estimated Maunder Minimum reductions in the bands, compared with that of Lean (2000).

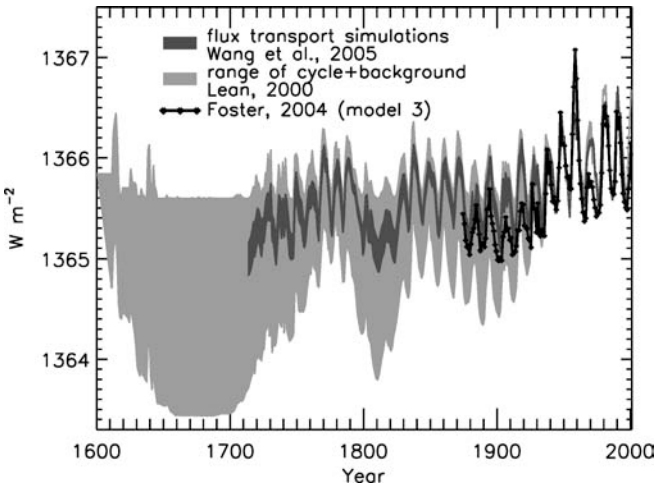

Figure 10. Shown as the upper envelope of the shaded region are total solar irradiance variations arising from the 11-year activity cycle. The lower envelope is the total irradiance reconstructed by Lean (2000), in which the long-term trend was inferred from brightness changes in Sun-like stars. In comparison are recent reconstructions based on solar considerations alone. That of Wang, Lean, and Sheeley (2005) uses a flux transport model to simulate the long-term evolution of the closed flux that generates bright faculae.

3.2.3. *Future*

Solar irradiance is expected to continue cycling in response to the 11-year activity cycle. Figure 12 suggests a possible scenario for the next few decades, based on a linear relationship of annual mean irradiance with the 10.7 cm flux (Lean, 2001). Predictions of the 10.7 cm flux, made by Schatten (2003) use a precursor approach that invokes solar dynamo theory to forecast cycle maxima from the strength of the Sun's polar fields at minima.

The prediction in Figure 12 has large uncertainty, in part because total solar irradiance is not linearly related to solar activity. Rather, its amplitude is the net effect of sunspot darkening and facular brightening, both of which vary with solar activity. Notably, total solar irradiance was as high in cycle 23 as in the prior two cycles, even though solar activity was not. Additionally, the irradiance database is too short for the detection or understanding of long-term solar irradiance trends that may also affect future radiative output.

That current levels of solar activity are at overall high levels, according to both the sunspot numbers and cosmogenic isotopes, may imply that future solar irradiance values will not exceed significantly those in the contemporary database. Spectral synthesis of the cosmogenic isotope record confirms that solar activity is presently peaking, and in 2100 will reach levels comparable to those in 1990 (Clilverd *et al.*, 2003). Projections of combined 11-, 88-, and 208-year solar cycles also suggest that solar activity will increase in the near future, until 2030, followed by decreasing

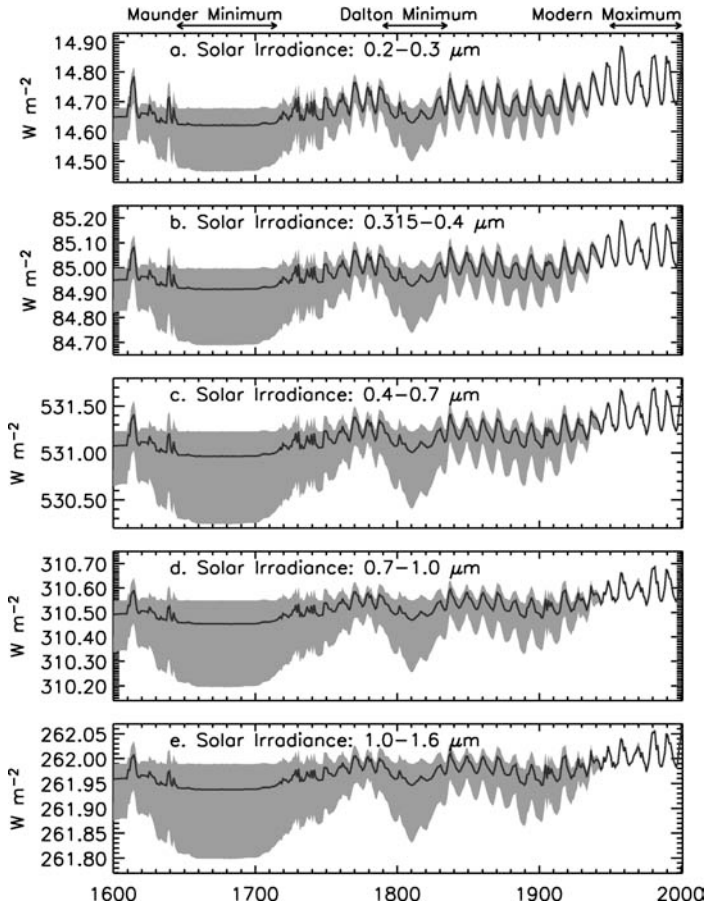

Figure 11. The shaded region shows the range of spectral irradiance variations in five wavelength bands, from the 11-year activity cycle alone to the estimate of Lean (2000), in which the long-term trend was inferred from brightness changes in Sun-like stars. In comparison are new irradiance reconstructions based on solar considerations alone, by Wang, Lean, and Sheeley (2005), using a flux transport model to simulate the long-term evolution of the closed flux that generates bright faculae.

activity until 2090 (Jirikowic and Damon, 1994). In contrast, a numerical model of solar irradiance variability which combines cycles related to the fundamental 11-year cycle by powers of 2 predicts a 0.05% irradiance decrease during the next two decades (Perry and Hsu, 2000).

SORCE's irradiance observations during the upcoming activity minimum (predicted for 2007) and cycle 24 activity maximum (predicted for 2010) will provide unique observations crucial for understanding the relationship of irradiance to solar activity, and for clarifying activity minima levels that may help resolve the controversy introduced by the different composite time series in Figure 4. Noting that radiometer sensitivities degrade most quickly during the beginning of the mission

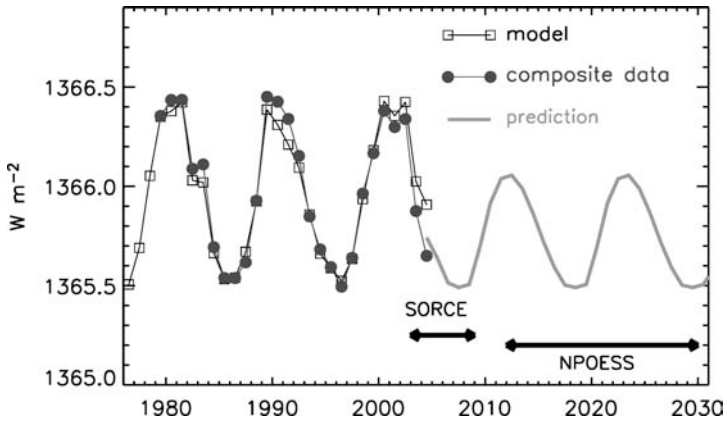

Figure 12. Predicted variations of total solar irradiance are shown during upcoming solar cycles, based on the Schatten (2003) predicted 10.7 cm flux. Also indicated is the expected epoch of operational monitoring by NPOESS, during which time solar activity may be notably less than during the present.

and that the NPOESS observations will commence in the declining phase of cycle 24, it will be essential to have independent monitoring by heritage radiometers during that time period.

4. Summary

Increasingly sophisticated statistical studies of high-fidelity climate, atmospheric, and solar variability time series in recent decades are contributing new knowledge of the Sun's influence on global change. Empirical evidence indicates surface and lower tropospheric temperature changes of order 0.1 K (peak-to-peak) associated with the solar activity cycle. The solar signal strength grows with altitude, to 1 K at 50 km. Changes in rainfall patterns in tropical regions also exhibit solar cycle periodicities, as do atmospheric ozone concentrations. Multiple regression analysis suggests that the solar influence on global change from solar minimum to maximum is comparable to anthropogenic effects over the same 5-year interval. Superimposed on both the cycling solar signal and the monotonically increasing anthropogenic influence are additional variations arising from internal variability and volcanic eruptions. When the contemporary empirical relationships are extended to the past 120 years, the solar influence on global surface temperature, consistent with current understanding of plausible secular irradiance change, is likely an order of magnitude smaller than the net warming from increasing concentrations of greenhouse gases and tropospheric aerosols.

The apparent surface temperature response to the solar activity cycle is inconsistent with current assumptions that the thermal inertia of the ocean attenuates the decadal solar forcing by a factor of 5. Efforts are underway to conduct more

realistic response scenarios, by extending the upper boundary of general circulation models to above the stratosphere, improving ozone chemistry parameterizations, and using spectral, rather that total, irradiance inputs. Simulations with these expanded models suggest that solar effects on ozone and winds may propagate into the troposphere, and may influence the NAO. Recent approaches have used a regional model to explore ENSO responses to direct solar forcing and a stratospheric model to simulate changes in QBO phase caused by the UV irradiance cycle, but these mechanisms have yet to be included in general circulation models.

Reliable solar irradiance time series are crucial for both empirical and model investigations. Thus far, most studies have used the total solar irradiance record which extends since late 1978. SORCE observations by TIM continue this database. A critical, independent radiometric assessment of the space-based datasets is necessary to resolve radiometric differences of order $5\,\mathrm{Wm}^{-2}$ between SORCE and prior observations. Also needed is radiometric assessment of sensitivity drifts in the Nimbus 7 radiometer whose measurements between 1989 and 1992 are the basis for surmising that solar irradiance has increased between the two recent solar minima in 1986 and 1996. In comparison, overlapping ERBS observations and model simulations based on sunspot and facular influences do not show such an increase. The possibility of mistaking instrumental effects for real secular irradiance change emphasizes the need for continuing, overlapping measurements by independent radiometers to obtain a properly cross-calibrated long-term record of solar irradiance.

SORCE's SIM measurements realize the first continuous monitoring of variations in the near-UV, visible, and near-IR regions of the solar spectrum. This new database of spectral irradiance changes will enable more realistic investigations of the mechanisms of climate responses to solar forcing. The SORCE spectral irradiance observations are being examined to better quantify the sources of irradiance variability and the spectral partitioning of the variations. Empirical models of present and past solar irradiance variations, which utilize parameterizations of sunspot and facular influences, are being revised. Differences already detected include the apparent underestimation of the facular and sunspot influences, especially of the facular brightness in the near-IR regions. More physical approaches for modeling solar irradiance variations are also underway and may lead to better understanding of plausible longer term changes such as during the Maunder Minimum. SORCE's observations during the upcoming activity minimum (in 2007) and cycle 24 maximum (2010) will provide crucial benchmark data.

Acknowledgements

NASA and ONR funded this work. The efforts of the SORCE team in acquiring and reducing the data are appreciated, especially the help of Chris Pankratz. Ken Schatten provided solar cycle predictions. Bill Livingston and Rodney Viereck

provided proxies to update the irradiance variability model. Mike Lockwood provided recent estimates of long-term irradiance changes. Gratefully acknowledged are discussions with Claus Fröhlich, David Rind, and Yi-Ming Wang. Additional data were obtained from the MDI, NGDC, GISS, GSFC, NOAA, and JMA websites.

References

Allen, C. W.: 1981, *Astrophysical Quantities*, 3rd edn, The Athlone Press, University of London.
Baliunas, S. and Jastrow, R.: 1990, *Nature* **348**, 520.
Baud, E., Raisbeck, G., Yiou, F., and Jouzel, J.: 2000, *Tellus* **52B**, 985.
Bond, G., Kromer, B., Beer, J., Muscheler, R., Evans, M. N., Showers, W., Hoffmann, S., Lotti-Bond, R., Hajdas, I., and Bonani, G.: 2001, *Science* **294**, 2130.
Clilverd, M. A., Clarke, E., Rishbeth, H., Clark, T. D. G., and Ulich, T.: 2003, *Astron. Geophys.* **44**, 2025.
Coughlin, K. and Tan, K. K.: 2004, *J. Geophys. Res.* **109**, D21105.
Crowley, T.: 2000, *Science* **289**, 270.
Dewitte, S., Crommelynck, D., Mekaoui, S., and Joukoff, A.: 2005, *Solar Phys.* **224**, 209.
Donarummo, J., Jr., Ram, M., and Stolz, M. R.: 2002, *Geophys. Res. Lett.* **29**, 75.
Douglass, D. H. and Clader, B. D.: 2002, *Geophys. Res. Lett.* **29**, 33.
Fioletov, V. E., Bodeker, G. E., Miller, A. J., McPeters, R. D., and Stolarski, R.: 2002, *J. Geophys. Res.* **107**, D22.
Fligge, M. and Solanki, S. K.: 2000, *Geophys. Res. Lett.* **27**, 2157.
Fontenla, J., White, O. R., Fox, P. A., Avrett, E. H., and Kurucz, R. L.: 1999, *Astrophys. J.* **518**, 480.
Fontenla, J. M., Harder, J., Rottman, G., Woods, T., Lawrence, G. M., and Davis, S.: 2004, *Astrophys. J.* **605**, L85.
Foster, S. S.: 2004, Ph.D. thesis, School of Physics and Astronomy, Faculty of Science, University of Southampton.
Foukal, P., North, G., and Wigley, T.: 2004, *Science* **306**, 68.
Fröhlich, C. and Lean, J.: 2004, *Astron. Astrophys. Rev.* **12**, 273.
Geller, M. and Smyshlyaev, S.: 2002, *Geophys. Res. Lett.* **29**, 5.
Gleisner, H. and Thejll, P.: 2003, *Geophys. Res. Lett.* **30**, 942.
Haigh, J. D.: 2001, *Science* **294**, 2109.
Haigh, J. D.: 2003, *Philos. Trans. R. Soc.* **361**, 95.
Haigh, J. D., Austin, J., Butchart, N., Chanin, M.–L., Crooks, S., Gray, L. J., Halenka, T., Hampson, J., Hood, L. L., Isaksen, I. S. A., Keckhut, P., Labitzke, K., Langematz, U., Matthes, K., Palmer, M., Rognerud, B., Tourpali, K., and Zerefos, C.: 2004, *SPARC Newslett.* **23**, 19.
Hall, J. C. and Lockwood, G. W.: 2004, *Astrophys. J.* **614**, 942.
Hansen, J.: 2004, *Sci. Amer.* **290**, 68.
Hansen, J., Sato, M., Nazarenko, L., Ruedy, R., Lacis, A. et al.: 2002, *J. Geophys. Res.* **107**, 4347.
Harder, J., Lawrence, G., Fontenla, J., Rottman, G., and Woods, T.: 2005, *Solar Phys.*, this volume.
Hood, L.: 2003, *Geophys. Res. Lett.* **30**, 10.
Hoyt, D. V. and Schatten, K. H.: 1993, *J. Geophys. Res.* **98**, 18895.
Intergovernmental Panel on Climate Change, Third Assessment Report: 2001.
Jackman, C., Flemming, E., Chandra, S., Considine, D., and Rosenfield, J.: 1996, *J. Geophys. Res.* **101**, 753.
Jirikowic, J. L. and Damon, P. E.: 1994, *Clim. Change* **26**, 309.
Jones, P. and Mann, M.: 2004, *Rev. Geophys.* **42**, RG2002.
Kernthaler, S. C., Toumi, R., and Haigh, J. D.: 1999, *Geophys. Res. Lett.* **26**, 863.

Kiehl, J. T. and Trenberth, K. E.: 1997, *Bull. Amer. Meteorolog. Soc.* **78,** 197.
Kodera, K.: 2002, *Geophys. Res. Lett.* **29**, 1218.
Kodera, K.: 2004, *Geophys. Res. Lett.* **31**, L24209.
Kopp, G., Lawrence, G., and Rottman, G.: 2005, *Solar Phys.*, this volume.
Kristjánsson, J. E., Staple, A., Kristiansen, J., and Kaas, E.: 2002, *Geophys. Res. Lett.* **29**, 22.
Krivova, N. A., Solanki, S. K., Fligge, M., and Unruh, Y. C.: 2003, *Astron. Astrophys.* **399**, L1.
Kuhn, J. R., Lin, H., and Coulter, R.: 1999, *Adv. Space Res.* **24/2**, 185.
Labitzke, K.: 2004, *J. Atmos. Solar-Terrest. Phys.* **66**, 1151.
Lacis, A. A., Wuebbles, D. J., and Logan, J. A.: 1990, *J. Geophys. Res.* **95**, 9971.
Lean, J.: 2000, *Geophys. Res. Lett.* **27**, 2425.
Lean, J.: 2001, *Geophys. Res. Lett.* **28**, 4119.
Lean, J., Beer, J., and Bradley, R.: 1995, *Geophys. Res. Lett.* **22**, 3195.
Lean, J., Wang, Y.-M., and Sheeley, N. R., Jr.: 2002, *Geophys. Res. Lett.* **29**, 77.
Lean, J., Skumanich, A., and White, O.: 1992, *Geophys. Res. Lett.* **19**, 1595.
Lean, J. L., Rottman, G. J., Kyle, H., Woods, T. N., Hickey, J. R., and Puga, L. C.: 1997, *J. Geophys. Res.* **102**, 29939.
Lean, J. L., Cook, J., Marquette, W., and Johannesson, A.: 1998, *Astrophys. J.* **492**, 390.
Lee III, R. B., Gibson, M. A., Wilson, R. S., and Thomas, S.: 1995, *J. Geophys. Res.* **100**, 1667.
Lockwood, M. and Stamper, R.: 1999, *Geophys. Res. Lett.* **26**, 2461.
Mann, M. E., Cane, M. A., Zebiak, S. E., and Clement, A.: 2005, *J. Climate* **18**, 447.
Matthes, K., Langematz, U., Gray, L. L., Kodera, K., and Labitzke, K.: 2004, *J. Geophys. Res.* **109**, D66101.
McClintock, W. E., Rottman, G. J., and Woods, T. N.: 2005, *Solar Phys.*, this volume.
McCormack, J.: 2003, *Geophys. Res. Lett.* **30**, 6.
McCormack, J. P., Hood, L. L., Nagatani, R., Miller, A. J., Planet, W. G., and McPeters, R. D.: 1997, *Geophys. Res. Lett.* **24**, 2729.
Meehl, G. A., Washington, W. M., Wigley, T. M. L., Arblaster, J. M., and Dai, A.: 2003, *J. Clim.* **16**, 426.
Neelin, J. D. and Latif, M.: 1998, *Phys. Today*, December.
Perry, C. A. and Hsu, K. J.: 2000, *PNAS* **97**, 12433.
Pilewskie, P. and Rottman, G.: 2005, *Solar Phys.*, this volume.
Preminger, D. G., Walton, S. R., and Chapman, G. A.: 2002, *J. Geophys. Res.* **107**, 1354.
Rial, J. A.: 1999, *Science* **285**, 564.
Rind, D.: 2002, *Science* **296**, 673.
Rind, D. and Overpeck, J.: 1993, *Quat. Sci. Rev.* **12**, 357.
Rind, D., Lonergan, P., Lean, J., Shindell, D., Perlwitz, J., Lerner, J., and McLinden, C.: 2004, *J. Clim.* **17**, 906.
Rottman, G.: 2005, *Solar Phys.*, this volume.
Rottman, G., Harder, J., Fontenla, J., Woods, T., White, O., and Lawrence, G.: 2005, *Solar Phys.*, this volume.
Ruzmaikin, A.: 1999, *Geophys. Res. Lett.* **26**, 2255.
Ruzmaikin, A. and Feynman, J.: 2002, *J. Geophys. Res.* **107**, D14.
Salby, M. and Callaghan, P.: 2004, *J. Clim.* **17**, 34.
Sato, M., Hansen, J. E., McCormick, M. P., and Pollack, J. B.: 1993, *J. Geophys. Res.* **98**, 22987.
Schatten, K. H.: 2003, *Adv. Space Res.* **32**, 451.
Schatten, K. H. and Orosz, J. A.: 1990, *Solar Phys.* **125**, 179.
Shindell, D. T., Schmidt, G. A., Miller, R. L., and Mann, M. E.: 2003, *J. Clim.* **16**, 4094.
Solanki, S. K. and Krivova, N. A.: 2004, *Solar Phys.* **224**, 197.
Solanki, S. K. and Unruh, Y. C.: 1998, *Astron. Astrophys.* **329**, 747.
Svalgaard, L., Cliver, E. W., and Le Sager, P.: 2004, *Adv. Space Res.* **34**, 436.

Tett, S. F. B., Jones, G. S., Stott, P. A., Hill, D. C., Mitchell, J. F. B., Allen, M. R., Ingram, W. J., Johns, T. C., Johnson, C. E., Jones, A., Roberts, D. L., Sexton, D. M. H., and Woodage, M. J.: 2002, *J. Geophys. Res.* **107**, 4306.

Udelhofen, P. N. and Cess, R. D.: 2001, *Geophys. Res. Lett.* **28**, 13.

Usoskin, I. G., Marsh, N., Kovaltsov, G. A., Mursula, K., and Gladysheva, O. G.: 2004, *Geophys. Res. Lett.* **31**, 16.

van Loon, H. and Shea, D. J.: 2000, *Geophys. Res. Lett.* **27**, 2965.

van Loon, H., Meehl, G. A., and Arblaster, J. M.: 2004, *J. Atmos. Solar-Terrest. Phys.* **66**, 1767.

Viereck, R. A., Floyd, L. E., Crane, P. C., Woods, T. N., Knapp, B. G., Rottman, G., Weber, M., and Puga, L. C.: 2004, *Space Weather* **2**, S10005.

Wallace, J. M. and Thompson, D. W. J.: 2002, *Phys. Today*, February.

Walton, S. R., Preminger, D. G., and Chapman, G. R.: 2003, *Astrophys. J.* **590**, 1088.

Wang, Y.-M., Lean, J. L., and Sheeley, N. R., Jr.: 2005, *Astrophys. J.* **625,** 522.

White, W. B., Dettinger, M. D., and Cayan, D. R.: 2003, *J. Geophys. Res.* **108**, 3248.

Wigley, T. M. L. and Raper, S. C. B.: 1990, *Geophys. Res. Lett.* **17**, 2169.

Willson, R. C. and Mordvinov, A. V.: 2003, *Geophys. Res. Lett.* **30**, 3.

Wolter, K. and Timlin, M. S.: 1998, *Weather* **53**, 315.

Woods, T. N. and Rottman, G.: 2005, *Solar Phys.*, this volume.

Woods, T. N., Prinz, D. K., Rottman, G. J., London, J., Crane, P. C., Cebula, R. P., Hilsenrath, E., Brueckner, G. E., Andrews, M. D., White, O. R., VanHoosier, M. E., Floyd, L. E., Herring, L. C., Knapp, B. G., Pankratz, C. K., and Reiser, P. A.: 1996, *J. Geophys. Res.* **101**, 9541.

Woods, T. N., Eparvier, F. G., Bailey, S. M., Chamberlin, P. C., Lean, J., Rottman, G. J., Solomon, S. C., Tobiska, W. K., and Woodraska, D. L.: 2005, *J. Geophys. Res.* **110**, A01312.